

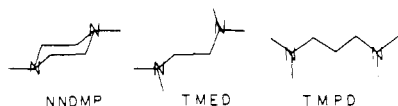
Structural Effects on Photophysical Properties in Saturated Amines. IV. Intramolecular Excimer Formation^{1,2b}

Arthur M. Halpern*^{2a} and P. P. Chan

Contribution from the Photochemistry and Spectroscopy Laboratory, Department of Chemistry, Northeastern University, Boston, Massachusetts 02115. Received September 30, 1974

Abstract: The fluorescence properties of two saturated diamines, *N,N,N',N'*-tetramethylethylenediamine (TMED) and *N,N,N',N'*-tetramethyl-1,3-propanediamine (TMPD), are compared with another diamine, *N,N'*-dimethylpiperazine (NNDMP), and a monoamine, trimethylamine (TMA). It is concluded that for the diamines studied, the lowest excited state is characterized by an interaction between the two nitrogen centers. The absorption spectra and the ionization potential values of the diamines are very similar to the respective properties of TMA. The fluorescence maxima of the diamines, however, are red shifted relative to monoamines, and, more significantly, the radiative rate constants for the diamines, k_R , are all considerably smaller than that for TMA. These data are interpreted in terms of these diamines as having lowest excited states which are excimeric nature; i.e., these states are not directly reachable via a radiative transition from the ground state(s). For TMED, the pressure dependence of ϕ_f and the decay curves have been analyzed from ca. 0.05 Torr to ca. 12 Torr. From these data, eight rate constants have been elucidated which characterize the dynamic properties of the excited state. It was found that the radiative rate constant of the relaxed (excimeric) state was pressure dependent, having a pressure coefficient of ca. 2.4×10^9 ($M^{-1} \text{ sec}^{-1}$). The vapor phase fluorescence spectrum of TMPD is very sensitive to excitation wavelength; two distinct emission bands can be observed. One band at 290 nm is assigned as monomer fluorescence, and the other at 365 nm is interpreted as the excimer emission spectrum. In a condensed medium, the ratio of the excimer-monomer intensities exhibits the usual temperature dependence. The binding energy of the TMPD intramolecular excimer is ca. 2.7 kcal/mol.

In a previous paper, the photophysical properties of the symmetrically bifunctional amine, *N,N'*-dimethylpiperazine (NNDMP), were examined and compared with those of several monoamines.³ On the basis of the spectral properties of this diamine, as well as the value of its radiative rate constant, it was concluded that the nonbonding orbitals centered on the nitrogen atoms became coupled in the excited (singlet) state. This paper is one of a series dealing with the symmetrical cage amines 1-azabicyclo[2.2.2]octane (ABCO), 1,4-diazabicyclo[2.2.2]octane (DABCO), and structurally analogous compounds. This work reports the results of a further investigation of the photophysical properties of two related diamines: *N,N,N',N'*-tetramethylethylenediamine (TMED) and *N,N,N',N'*-tetramethyl-1,3-propanediamine (TMPD). Both NNDMP and TMED bear a



formal resemblance to the rigid bicyclic cage amine 1,4-diazabicyclo[2.2.2]octane (DABCO), in which one (two) of the ethylene bridges is (are), respectively, opened. In DABCO, the fixed orientation of the two nitrogen atoms results in ground state interaction⁴⁻⁶ with the consequent absorptive⁷ and emissive⁸ spectroscopic characteristics.

Spectroscopic Properties

The vapor phase absorption spectra of TMED and TMPD, like NNDMP, resemble that of a monofunctional amine, e.g., trimethylamine (TMA). For example, the ϵ_{max} values are very similar. Furthermore, ϵ_{max} values of TMED ($7540 M^{-1} \text{ cm}^{-1}$) and TMPD ($6470 M^{-1} \text{ cm}^{-1}$) are roughly twice that of TMA ($3460 M^{-1} \text{ cm}^{-1}$). It should be realized that in the nonrigid tertiary amines, the absorption band (which is structureless) at ca. 195–200 nm corresponds to the $S_2 \leftarrow S_0$ transition. TMA is the only amine in this class for which the $S_1 \leftarrow S_0$ transition is discernible, having a shoulder at ca. 227 nm. At this wavelength, another

quantitative comparison can be made. ϵ (227 nm) for TMED and TMA is respectively 2150 and $910 M^{-1} \text{ cm}^{-1}$, again in a ratio of about 2:1. These spectroscopic data are summarized in Table I.

Photoelectron spectroscopic data of TMED⁹ provide another basis of comparison with other amines. The vertical ionization potential (IP) of 8.34 eV is close to the IP's of both NNDMP³ and TMA:¹⁰ 8.41 and 8.5 eV, respectively. These data as well as the optical spectroscopic data imply that in the diamines TMED and NNDMP, the nonbonding orbitals are unsplit by any ground state coupling.¹¹ It seems therefore a good approximation to view these two diamines as noninteracting bonded dimers of TMA. The IP values for these amines are also contained in Table I.

The emission properties of TMA, TMED, TMPD, and NNDMP, on the other hand, are rather dissimilar. The fluorescence spectra of TMED and NNDMP maximize at 304 and 313 nm, respectively, while λ_{max} for TMA is at 287 nm. λ_{max} for TMPD is 365 nm. The fluorescence properties of TMPD will be discussed below. More striking differences are encountered in the comparison of the radiative rate constants (k_R) of these amines. The k_R values are contained in Table I along with the zero-pressure lifetime and (absolute) quantum yield values. Whereas k_R for TMA ($2.1 \times 10^7 \text{ sec}^{-1}$) is typical for a monoamine, the k_R values for the diamines are significantly smaller (although k_R for TMED is about ten times greater than that for NNDMP). The wide difference in the k_R values of these diamines will be discussed below. Figures 1 and 2 respectively show the absorption and emission spectra of TMED and TMPD (vapor) at ambient temperature.

The diamines also differ from TMA with respect to their fluorescence decay characteristics. TMA fluorescence follows simple (first-order) decay kinetics at all pressures above 1 Torr (for $\lambda_{\text{exc}} > \text{ca. } 230 \text{ nm}$). On the other hand, the fluorescence decay properties of NNDMP are rather complicated (see ref 3). TMED is also characterized by nonexponential decay kinetics at all pressures examined (0.3–15.5 Torr) and at all exciting wavelengths used (up to

Table I. Summary of Spectroscopic and Fluorescence Data of Amines

Amine	λ_{\max} , nm	ϵ_{\max} , $M^{-1} \text{ sec}^{-1}$	IP, eV	λ_{\max} (fluor) nm	$\tau_{p \rightarrow o^a}$ (nsec)	$\phi_{p \rightarrow o^a}$	$k_R,^a \text{ sec}^{-1}$
TMA	198	3460	8.5	287	45	1.0	2.1×10^7
TMED	195	7540	8.34	304	71	0.23 ^b	3.2×10^6
NNDMP	205	6800	8.41	313	770	0.23	3.2×10^5
TMPD	202	6470		365	42	0.11 ^c	2.6×10^6

^a Values refer to the vibrationally relaxed lowest excited state. ^b Calculated from $k_{R1}/(k_{R1} + k_{NR1})$, see Figure 6. ^c Obtained from a ϕ_f measured at 5.0 Torr; $\phi_{p \rightarrow o}$ calculated by extrapolation using $k_Q = 8.5 \times 10^9 M^{-1} \text{ sec}^{-1}$.

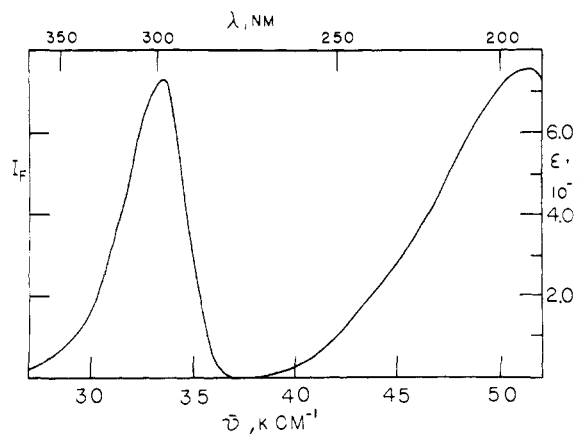


Figure 1. Vapor phase absorption and (corrected) emission spectra of 3.0 Torr of TMED in the presence of 100 Torr of *n*-hexane; $\lambda_{\text{exc}} = 265$ nm.

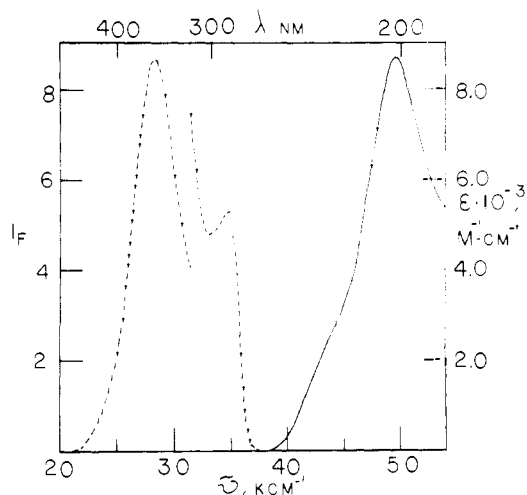


Figure 2. Vapor phase absorption and (uncorrected) emission spectra of 5.0 Torr of TMPD in the presence of 100 Torr of *n*-hexane; $\lambda_{\text{exc}} = 238$ nm.

265 nm). The decay curve for TMED at 5.0 Torr with λ_{exc} of 265 nm is depicted in Figure 3. This decay curve can be represented by the following equation

$$I_t(t) \propto 0.70 \exp(-t/8.4) + 0.30 \exp(-t/51.0)$$

where t is nanoseconds. All of the TMED decay curves are analyzed in terms of two exponential components. For future reference, τ_s and τ_l refer respectively to the short- and long-lived emission components. A plot of $1/\tau_l$ vs. TMED pressure, shown in Figure 4, is linear and provides values of the zero-pressure lifetime and the self-quenching constant (vide infra). At a given TMED pressure, the value of the long-lived component was independent of excitation wavelength ($230 < \lambda_{\text{exc}} < 265$ nm). However, as λ_{exc} was decreased, the amplitude of the short-lived component increased. This was accompanied by a strong decrease in the value of τ_s .

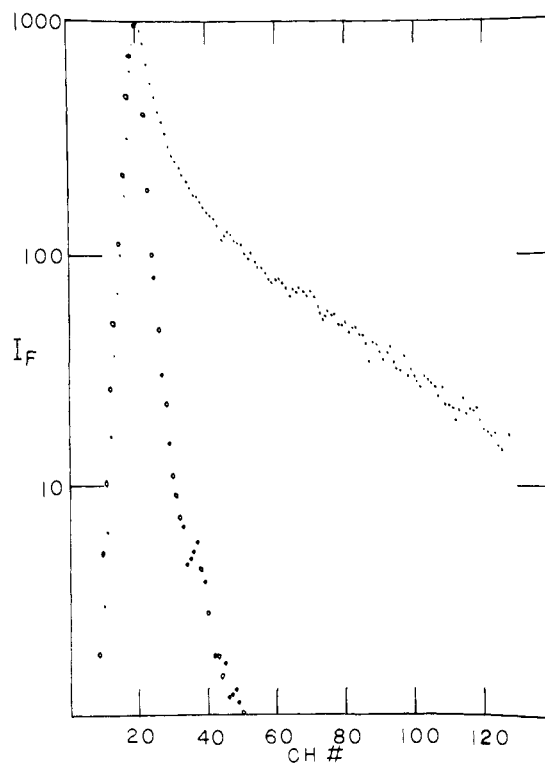


Figure 3. Fluorescence decay curve of TMED vapor (5.0 Torr). The exciting wavelength is 265 nm (1.6 nm bandpass), and the channel width is 1.29 nsec. Open circles correspond to the flash lamp profile.

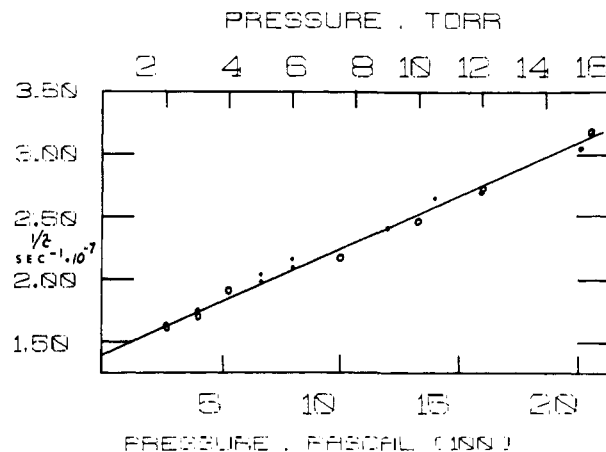


Figure 4. Plot of the reciprocal of the long-lived component (τ_l) vs. TMED pressure. Closed circles refer to λ_{exc} of 265 nm; open circles refer to λ_{exc} of 250 nm.

The value of τ_l , as well as its relative amplitude, was examined at several pressures between 3 and 6 Torr of TMED, and with $\lambda_{\text{exc}} = 265$ nm. It is over this pressure range that these decay parameters could be most accurately obtained. The pressure dependence of the short-lived component implies that collisions between excited state and ground state TMED molecules are extremely efficient in

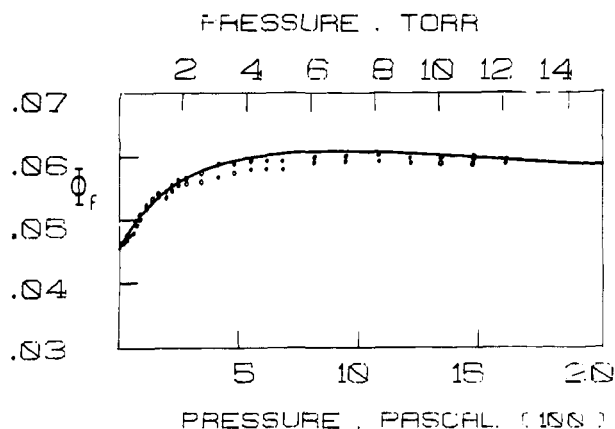


Figure 5. Plot of the absolute emission quantum yield vs. TMED pressure. The points refer to the experimental data, and the line is computed from the $\phi_f(A)$ expression given in the text. The rate constants used are contained in Table II.

depopulating the state from which the short-lived fluorescence emanates. This will be discussed below.

Unlike NNDMP,³ the fluorescence spectrum of TMED is invariant with excitation wavelength ($238 < \lambda_{\text{exc}} < 265$ nm). However, after irradiation at 238 nm¹² for several minutes, the fluorescence spectrum changed, becoming that produced by a photoproduct. This fluorescent product was readily identified as TMA through its characteristic fluorescence spectrum.^{13,14} After about 20 min of irradiation at 238 nm, the dominant emission spectrum observed was that due to TMA. No attempt was made to analyze the other photoproduct(s). Presumably the TMA is formed subsequent to the homolytic dissociation of the C-C bond in TMED. No TMA emission was produced if the TMED was irradiated at 265 nm for an appropriate time period such that the same amount of light was absorbed relative to 238 nm excitation.¹⁵ This observation suggests that there is a rather strong energy dependence to the photodissociation process, and it is consistent with this that the fluorescence quantum yield was found to decrease very sharply between 265 and 238 nm. For example, at 5 Torr TMED pressure, ϕ_f decreases by a factor of ca. 30 between λ_{exc} of 265 and 238 nm.

Quantum Yield Measurements

In order to avoid the complication due to photoproduct formation, quantum yield experiments were carried out at 265 nm (about 37.8 kcm^{-1}). It can be seen in Figure 1 that this frequency lies at the extreme low-energy end of the TMED absorption system (at this position $\epsilon = 21.2 \text{ M}^{-1} \text{ cm}^{-1}$). The relative quantum yield of TMED emission was measured as a function of pressure over the range of 0.1 Torr to ca. 12 Torr. Inner filter effects were neglected because at the maximum pressure reached, the optical density is only 0.0136. The absolute quantum yield was then obtained by comparisons with TMA vapor at several pressures (see Experimental Section). The TMA was corrected for self quenching.^{3,16}

The pressure dependence of ϕ_f is shown in Figure 5. Qualitatively, the increase in ϕ_f at low pressures (up to ca. 4 Torr) can be explained in terms of vibrational relaxation and fluorescence enhancement. After reaching a plateau at ca. 4 Torr, however, ϕ_f remains nearly constant up to about 12 Torr despite the fact that the amine undergoes self quenching (vide supra). Model calculations indicate that even with fluorescence enhancement (via vibrational relaxation), ϕ_f should start to decrease at higher pressure. The failure to observe the decrease in ϕ_f implies that (1) vibra-

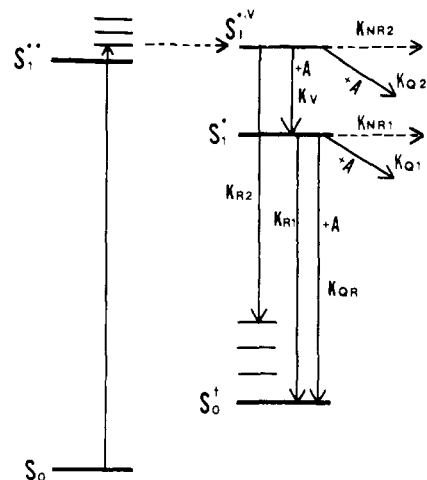


Figure 6. Schematic state diagram for TMED.

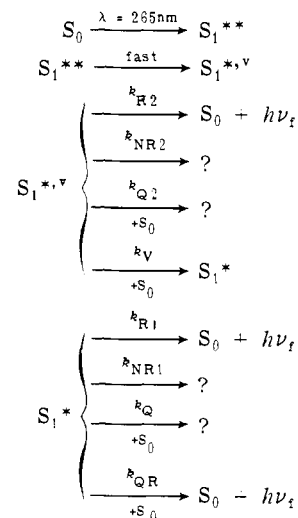
tional relaxation is relatively inefficient or that (2) there is a pressure dependence to k_R . The former possibility is discounted on the basis of the available kinetic (decay curve) data, and therefore the second possibility will be taken as a working hypothesis. Thus k_R for (vibrationally relaxed) TMED is expressed as follows

$$k_R = k_{R1} + k_{QR}[A]$$

where k_{R1} is the radiative rate constant at zero pressure, k_{QR} is the (bimolecular) radiative "quenching" rate constant, and $[A]$ is the concentration of the amine vapor (in M). Using the above expression for k_R , and incorporating the rate constants obtained from transient measurements, an attempt was made to calculate ϕ_f as a function of pressure, and to fit the data depicted in Figure 5.

By including k_{QR} in the expression of $\phi_f[A]$, the experimental data could be reasonably well accounted for at pressures above about 5 Torr. Below 5 Torr, however, it was necessary to include additional rate constants and thus to modify the photophysical mechanism. The basic scheme from which the $\phi_f[A]$ expression was derived is one containing two emissive states which are coupled via (bimolecular) vibrational relaxation. A schematic state diagram which represents the TMED system is portrayed in Figure 5, and the kinetic mechanism which pertains to this scheme is in Scheme I.

Scheme I



The rate constants employed in Scheme I are defined in Table II. Referring to Figure 6, S_0 denotes the TMED

Table II. Definition and Values of Rate Constants

Rate constant	Definition ^a	Value
k_{R_2}	Radiative rate constant of unrelaxed state ($S_1^{*,v}$)	$3.5 \times 10^6 \text{ sec}^{-1}$
k_{NR_2}	Nonradiative rate constant of $S_1^{*,v}$	$6.8_5 \times 10^7 \text{ sec}^{-1}$
k_{Q_2}	Quenching constant of $S_1^{*,v}$	$2.1_5 \times 10^{11} M^{-1} \text{ sec}^{-1}$
k_V	Vibrational relaxation constant of $S_1^{*,v}$	$1.2_5 \times 10^{11} M^{-1} \text{ sec}^{-1}$
k_{R_1}	Radiative rate constant of relaxed state (S_1^*)	$3.2 \times 10^6 \text{ sec}^{-1}$
k_{NR_1}	Nonradiative rate constant of S_1^*	$1.0_9 \times 10^7 \text{ sec}^{-1}$
k_{Q_1}	Quenching constant of S_1^*	$1.7_6 \times 10^{10} M^{-1} \text{ sec}^{-1}$
k_{QR}	Pressure coefficient of k_{R_1}	$2.4 \times 10^9 M^{-1} \text{ sec}^{-1}$

^a See Figure 6.

ground state, S_1^{**} refers to the lowest excited singlet state reached via absorption, $S_1^{*,v}$ is the initially formed (vibrationally excited) emissive state, and S_1^* corresponds to the vibrational relaxed emissive state.

The following important aspects of the proposed mechanism should be emphasized: (1) S_1^{**} is nonemissive; (2) S_1^{**} very rapidly ($<10^{-9}$ sec) converts to a lower lying, emissive excited state; and (3) two sublevels of S_1^* are fluorescent (the vibrationally excited and relaxed states). The basic experimental justifications for these assumptions are respectively: (1) exponential decay is observed if a sufficient overpressure of a buffer gas (*n*-hexane) is present and the fluorescence spectrum is independent of exciting wavelength (ignoring photochemical complications); (2) k_R values of the fluorescing states are very similar, yet both are much smaller than k_R for a monoamine; (3) the pressure dependencies of both ϕ_f and the decay curves are adequately accounted for in terms of only two emitting species.

From the mechanism described above, the following expression for $\phi_f[A]$ is readily derived.

$$\phi_f[A] = \frac{k_{R_2}}{k_{R_2} + k_{NR_2} + k_{Q_2}[A] + k_V[A]} + \left(\frac{k_V[A]}{k_{R_2} + k_{NR_2} + k_{Q_2}[A] + k_V[A]} \right) \times \left(\frac{k_{R_1} + k_{QR}[A]}{k_{R_1} + k_{NR_1} + k_{Q_1}[A] + k_{QR}[A]} \right)$$

$\phi_f[A]$ was computed for various sets of rate constants and compared with the experimental data. Certain rate constants were found to have appreciable influence over specific regions of the $\phi_f[A]$ plot. For example, k_{QR} was adjusted until the high-pressure portion of the plot was satisfactory. The exclusion of k_{QR} resulted in a sharp decrease in the theoretical values of ϕ_f in contradistinction to the trend observed in the experimental points.

At the low-pressure end of the plot (below 4 Torr), other rate constants greatly influenced the shape of the theoretical $\phi_f[A]$ plot (especially k_{Q_2} , k_V , and k_{R_2}). The solid line indicated in Figure 5 represents the best (empirical) fit to the experimental values of ϕ_f .

As a result of both kinetic (fluorescence decay) measurements and zero-pressure-limiting steady state (quantum yield) determinations, certain quantitative constraints are imposed upon various rate constants. These constraints are summarized in Table III along with their respective origins.

Table III. Summary of Constraints Imposed on Various Rate Constants

Constraint	Source
$k_{R_1} + k_{NR_1} = 1.41 \times 10^7 \text{ sec}^{-1}$	Intercept of $1/\tau_{\text{slow}}$ vs. pressure plot
$k_{Q_2} + k_{QR} = 2.0 \times 10^{10} M^{-1} \text{ sec}^{-1}$	Slop of above plot
$k_V + k_{Q_2} = 3.4 \times 10^{11} M^{-1} \text{ sec}^{-1}$	Pressure dependence of fast emission component
$(k_{R_1}/k_{R_2})k_V = 1.5 \times 10^{11} M^{-1} \text{ sec}^{-1}$	Ratio of amplitudes of slow and fast emission components
$k_{R_2} + k_{NR_2} = 7.5 \times 10^7 \text{ sec}^{-1}$	Zero pressure ϕ_f and τ_f values
$k_{R_2} = 3.5 \times 10^6 \text{ sec}^{-1}$	As above
$k_{NR_2} = 7.1 \times 10^7 \text{ sec}^{-1}$	As above

The values of the various rate constants finally adopted are listed in Table II, and it can be seen that they satisfy the requirements of the constraints within experimental error.

It can be seen from the data in Table II that the total cross section of $S_1^{*,v}$ with respect to deactivation, i.e., $k_{Q_2} + k_V$, is rather large ($3.4 \times 10^{11} M^{-1} \text{ sec}^{-1}$). This implies that this state is spacially extensive and also considerably reactive with respect to self quenching. Assuming that $3.4 \times 10^{11} M^{-1} \text{ sec}^{-1}$ represents the collision frequency of $S_1^{*,v}$ vis à vis S_0 , then vibrational relaxation takes place with roughly 30% efficiency.

One of the most unusual results to emerge from this study is the pressure dependence of k_R . This type of behavior (toward *n*-hexane as a buffer gas) has been noted before for other saturated amines,^{3,17,18} and thus, it appears that this k_R dependence may be a rather general characteristic of these systems. The excited state of the saturated amines (i.e., Rydberg type), being spacially extensive, would be expected to be quite sensitive to collisions with other molecules.^{7,19} It thus appears that the transition moment (e.g., the Einstein *A* coefficient) is augmented as a result of bimolecular interactions.

Another central outcome of this investigation is the suggestion that emission in TMED takes place from a lower lying excited state which is not directly reachable via radiative transitions from the ground state. It was mentioned above that a similar hypothesis was suggested in the case of NNDMP.³ An interesting, but equivalent, interpretation of the basic photophysical model can be sustained (refer to Figure 6). The excited state coupling between the two nitrogen atoms in TMED and NNDMP can be thought of as arising through the same type of excited state-ground state interaction such as in excimers. TMED and NNDMP would, then, correspond to intramolecular excimer systems. A more definitive assignment of the fluorescing states of these amines as intramolecular excimers would, however, require the elucidation of the usual kinetic and thermodynamic parameters of the monomer-excimer scheme.^{20,21} In TMED, the presumption that the (monomer-excimer) formation rate constant is very large (vide supra) precludes carrying out time-resolved studies of the monomer decay. In NNDMP, where dual luminescence is observed, kinetic studies of the monomer-excimer system could perhaps be pursued; presumably in this case also, the (first-order) formation rate constant is large.

It is interesting to consider what the configuration might be of the "coupled" excited state (S_1^*) of TMED (i.e., the excimer state). Presumably, the molecule adopts a conformation which allows some delocalization of the excitation energy to occur over the N-C-C-N atoms. One possible structure would be with the N-C-C-N dihedral angle close to 0° and with both of the methyl groups oriented away from each other. The destabilization which would result

Table IV. Excimer/Monomer Intensity Ratio (R) for TMPD in Various Saturated Hydrocarbon Solvents^a

Solvent	η , cP	R
<i>n</i> -Hexane	0.298	19.4
Cyclohexane	0.895	17.0
Hexadecane	3.086	14.2
Decalin		10.5
Vapor phase ^b		8.25

^a The TMPD concentration is 1×10^{-3} M, and λ_{exc} is 238 nm.
^b TMPD pressure is 5.0 Torr and ca. 150 Torr of *n*-hexane vapor is added.

from the eclipsing of the various C-H and *N*-methyl bonds would, presumably, be offset by the binding energy of the coupled state.

It should be noted that in the case of the intermolecular amine excimer, the arrangement of the two amine molecules appears to be in the head-to-head approach, i.e., with the nonbonding orbitals of the two nitrogen atoms facing each other.²² The structure proposed for TMED is analogous to this situation. One could rationalize the presumption that the (excimer) formation rate constant is very large because the structure suggested above is achieved by the rotation of the C-C and the C-N bonds. For such a process, a rate constant of $> 10^9$ is not unreasonable.

The fluorescence properties of TMPD will now be discussed. Since the vapor pressure of TMPD at 23° is about 5 Torr, extensive studies of the pressure dependence of the lifetime and quantum yield cannot be carried out. The limiting values of τ_f and ϕ_f at very low pressures (ca. 0.05 Torr) were determined and these data are contained in Table I. In TMPD, the disposition of the two amine monomers is such that intramolecular excimer formation (and stabilization) is rather dramatic as compared with NNDMP or TMED.

Like TMED and NNDMP, TMPD's absorption spectrum is quantitatively similar to that of a (double) monoamine. On the other hand, the fluorescence spectral and decay characteristics are unique. The vapor phase absorption and fluorescence spectra, shown in Figure 2, illustrate this point. λ_{max} (fluorescence), which is at 365 nm, is considerably lower in energy relative to a monoamine such as triethylamine ($\lambda_{\text{max}} = 282$ nm). The TMPD emission spectrum is also unusual in that it reveals a distinct shoulder at ca. 290 nm. This short wavelength component is not observed in the spectra of the diamines TMED and NNDMP. The 290-nm band is also evident in the fluorescence spectra of TMPD in various saturated hydrocarbon solvents. In the condensed phase, however, the ratio of the intensities [$\lambda(365)/\lambda(290)$], R , decreases as the solvent viscosity increases (e.g., from *n*-hexane to (cis and trans) decalin). In all cases, R when measured in a condensed medium is considerably larger than in the vapor phase (vide infra). These results are summarized in Table IV.

In the vapor phase, R is very sensitive to the excitation wavelength (if the total pressure of the system is low enough, e.g., < 10 Torr). As λ_{exc} is decreased, R strongly decreases. For example, when $\lambda_{\text{exc}} = 265$ nm, the TMPD spectrum is predominantly characterized by the 365 nm band, whereas for $\lambda_{\text{exc}} = 228$ nm, it is the 290 nm band which is almost exclusively observed. At intermediate excitation wavelengths, the emission spectrum is a composite of the 290 and 365 nm systems. Table V contains values of R corresponding to various excitation wavelengths. The fluorescence spectrum of TMPD is independent of excitation wavelength if a sufficient overpressure of a buffer gas is added. Under such conditions (e.g., 150 Torr of *n*-hexane), the 290 nm band is still observed, but the R value is much larger than the case without the buffer gas present (see

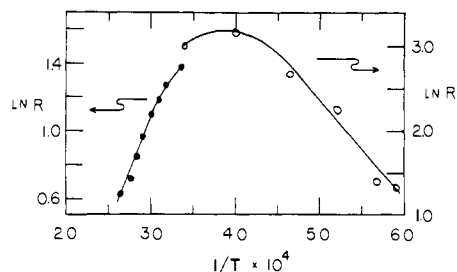


Figure 7. Plot of $\ln R$ vs. $1/T$ for 1×10^{-3} M solutions of TMPD in (cis and trans) decalin (left) and in methylcyclohexane-2-methylbutane (9:1) (right).

Table V. R Values for TMPD Vapor (5.0 Torr) at Different Excitation Wavelengths

λ_{exc} , nm	R	λ_{exc} , nm	R
228	0.13	249	1.03
238	0.324	265	3.72

Table IV).²³ The response of the fluorescence spectrum to the addition of a buffer gas (i.e., the λ_{exc} independence) confirms the fact that the 290 nm (or the 365 nm) emission band is not due to an impurity.

The 290 nm band is assigned as the emission from the excited monomer (i.e., the initially formed or uncoupled state), and the broad 365 nm band is interpreted as the emission from the TMPD intramolecular excimer (i.e., the coupled state). The essential difference between TMPD and TMED and NNDMP is that for the latter two diamines, emission from the excited monomer is not definitively observed. This is presumed to be the consequence of very large excimer-formation rate constants (k_{DM}) in these amines. In other words, k_{DM} in TMPD is, for various reasons, small enough to allow for the radiative relaxation of the excited monomer with a suitably high probability.²⁴

The temperature dependence of the emission spectrum (i.e., the variation of R with temperature) is consistent with the interpretation of intramolecular excimer formation in TMPD. The temperature dependence of R was examined in two different experiments: (1) using (cis and trans) decalin as the solvent, R was measured between 25 and ca. 100°; and (2) using methylcyclohexane (with ca. 10% v/v of 2-methylbutane) as the solvent medium, R was measured from ca. -100 to 25°. The TMPD concentration was 1×10^{-3} M. These results are displayed in Figure 7, in which $\ln R$ is plotted vs. $1/T$. In the low-temperature region (i.e., below ca. -25°), the slope of $\ln R$ is negative, whereas in the high-temperature region (i.e., above ca. -10°), the slope is positive. These data imply that at low temperature, the excimer-monomer ratio is determined by the activation energy pertaining to excimer formation (W_{DM}). At high temperatures, on the other hand, it is the difference in the activation energies of excimer dissociation and formation ($W_{\text{MD}} - W_{\text{DM}}$) which governs the excimer-monomer emission intensity ratio.²⁵ Thus, the limiting high- and low-temperature slopes are ($W_{\text{MD}} - W_{\text{DM}}$) and $-W_{\text{DM}}$, respectively. These activation parameters, obtained from the data shown in Figure 2, are: $W_{\text{DM}} \approx 2.3$ kcal/mol, and ($W_{\text{MD}} - W_{\text{DM}}$) ≈ 2.7 kcal/mol. The value of W_{DM} would, presumably, correlate with the trimethylene chain rotational barrier involved in excimer formation. Chandross and Dempster²⁶ have measured W_{DM} for the 1,3-bis(α -naphthyl)propane intramolecular excimer in a methylcyclohexane-2-methylbutane mixed solvent (9:1). Their value of 3.3 kcal/mol, which is larger than W_{DM} for the TMPD system, probably is a consequence of the fact that the α -naphthyl

moiety is bulkier than the dimethylamino group. Apparently, W_{DM} is not exclusively governed by the intramolecular rotational barriers associated with the trimethylene linkage. The solvent medium has been shown to play a role in determining certain activation parameters in the 1,3-bis(α -naphthyl)propane intramolecular excimer by El-Bayoumi et al.²⁷

The binding energy of the TMED excimer is equal to the activation energy difference ($W_{MD} - W_{DM}$), which is about 2.7 kcal/mol.²⁸ The fact that the TMPD emission spectrum is predominantly that of the excimer at room temperature (see Figure 2 and Table IV), despite such a low binding energy, is presumably a consequence of the more positive entropy of formation for an intramolecular excimer relative to the intermolecular case. This has been pointed out in ref 26. Kinetically, this would be manifest by either a larger value of k_{DM} and/or a smaller value of k_{MD} . Recently, El-Bayoumi et al.,²⁷ in studying the 1,3-bis(α -naphthyl)propane intramolecular excimer, have proposed that it is the dissociation rate constant (k_{MD}) which is retarded (relative to the naphthylene intermolecular excimer), resulting in a larger "equilibrium constant". Detailed kinetic and thermodynamic studies of TMPD and related diamines are in progress and the results will be reported in a forthcoming publication.

Experimental Section

TMED and TMPD, procured from Aldrich Chemical Co., were distilled in vacuo over CaH₂ and subsequently stored in the absence of oxygen. Purity was confirmed via GLC. Pressure measurements were carried out using a Baratron (MKS Instruments) with a Model 77 Pressure Head. Fluorescence spectra were obtained with a conventional dc fluorimeter described elsewhere.¹⁷ Fluorescence decay measurements were made using the time-correlated single photon technique.^{29,30} In certain cases, decay curves were convoluted with the exciting flashlamp profile according to a two component exponential decay model and then compared with the data to ensure parameter validity. Acquisition times were 2–10 hr. Calculations of the pressure dependence of ϕ_f were performed on a CDC-Cyber 72 computer and the results were displayed on an X-Y plotter (Time Share Peripherals Corp.) which was interfaced with the teletype.

The absolute quantum yields of TMED and TMPD were established using as the absolute standard the zero-pressure extrapolated value of ϕ_f for TMA of 1.0 with $\lambda_{exc} = 265 \text{ nm}$.³ The results of four determinations of ϕ_f , obtained with different pressures of both TMA and TMED, were averaged. The TMED pressures always exceeded 5 Torr, and the TMA fluorescence intensities were corrected for self quenching.³ Because of the low optical densities of these amines at 265 nm (over the pressures ranges used), inner filter effects were neglected. $\epsilon(265 \text{ nm})$ values are: 6.78 and 21.2 $M^{-1} \text{ cm}^{-1}$ for TMA and TMED, respectively. ϕ_f for TMPD was obtained by direct comparisons of the fluorescence intensity (at 5 Torr) with TMED.

The pressure dependence of ϕ_f for TMED and TMPD was determined ($\lambda_{exc} = 265 \text{ nm}$) by monitoring the fluorescence intensity (at 303 nm for TMED and 365 nm for TMPD) while the pressure of the amine was changed. For these measurements, the fluorescence cell was directly coupled to the vacuum system and pressure-reading apparatus. Identical results were obtained if the relative fluorescence intensity was derived by integrating the full fluorescence spectrum. Since inner filter effects were neglected, the relative fluorescence efficiency was obtained from $\phi_{rel} = I_f/P$, where I_f is the intensity and P is the TMED pressure.

References and Notes

- (1) (a) Part III: A. M. Halpern, *J. Am. Chem. Soc.*, **96**, 7655 (1974). (b) This research is supported by the National Science Foundation (Grant GP-43000-X).
- (2) (a) Alfred P. Sloan Research Fellow. (b) A portion of this research constitutes partial fulfillment of the M.S. degree of P.P.C.
- (3) A. M. Halpern and T. Gartman, *J. Am. Chem. Soc.*, **96**, 1393 (1974).
- (4) R. Hoffman, A. Imamura, and W. J. Hehre, *J. Am. Chem. Soc.*, **90**, 1499 (1968).
- (5) E. Heilbronner and K. A. Muszkat, *J. Am. Chem. Soc.*, **92**, 3813 (1970).
- (6) P. Bischof, J. A. Hashmall, E. Heilbronner, and V. Hornung, *Tetrahedron Lett.*, **No. 46**, 4025 (1969).
- (7) A. M. Halpern, J. L. Roebber, and K. Weiss, *J. Chem. Phys.*, **49**, 1348 (1967).
- (8) A. M. Halpern, *Chem. Phys. Lett.*, **6**, 296 (1970).
- (9) Professor J. L. Roebber and Dr. S. Khandelwal are gratefully acknowledged for their cooperation in obtaining the photoelectron spectrum of TMED.
- (10) A. B. Cornfield, D. C. Frost, F. G. Herring, and C. A. McDowell, *Can. J. Chem.*, **45**, 1135 (1971).
- (11) The photoelectron spectra of TMED and NNDMP indicate that the first transition (ionization from the n orbital) is rather broad: fwhm 0.86 and 0.72 eV, respectively. This may be indicative of weak splitting in the n orbitals.
- (12) A Hanovia 200-W dc Xe-Hg lamp was used with a 0.25-m Jarrel Ash monochromator (see ref 15).
- (13) A. M. Halpern, *Mol. Photochem.*, **5**, 517 (1973).
- (14) C. G. Freeman, M. J. McEwen, R. F. C. Clairidge, and L. F. Phillips, *Chem. Phys. Lett.*, **8**, 77 (1971).
- (15) With the light source used, the ratio of irradiation times for the same amount of light to be absorbed at 265 nm relative to 238 nm is ca. 23.2.
- (16) Assuming that k_R is a constant.
- (17) A. M. Halpern and R. M. Danziger, *Chem. Phys. Lett.*, **16**, 72 (1972).
- (18) A. M. Halpern, *J. Am. Chem. Soc.*, **96**, 4392 (1974).
- (19) M. B. Robin and N. A. Kuebler, *J. Mol. Spectrosc.*, **33**, 274 (1970).
- (20) J. B. Birks, "Photophysics of Aromatic Molecules", Wiley-Interscience, London, 1970, pp 301–305.
- (21) G. E. Johnson, *J. Chem. Phys.*, **61**, 3002 (1974).
- (22) A. M. Halpern and R. J. Sternfels, to be submitted for publication.
- (23) These effects can be interpreted in terms of vibrational relaxation within the excimer manifold and consequent fluorescence enhancement.
- (24) k_{DM} for TMPD, nevertheless, is rather large, 10^9 sec^{-1} .
- (25) See F. Hirayama and S. Lipsky, *J. Chem. Phys.*, **51**, 1939 (1969).
- (26) E. A. Chandross and C. J. Dempster, *J. Am. Chem. Soc.*, **92**, 3586 (1970).
- (27) P. Avouris, J. Kordas, and M. A. El-Bayoumi, *Chem. Phys. Lett.*, **26**, 373 (1974).
- (28) This represents a lower limit on the binding energy (which can also be expressed as $-\Delta H$) because, in actuality, the $\ln R$ vs. $1/T$ plot is curved (see Figure 7), and $d \ln R/d(1/T)$ approaches ΔH only in the limit of high temperature. Likewise, the value of W_{DM} given as 2.3 kcal/mol is to be construed as a lower limit. Activation parameters can be more accurately determined from kinetic rather than steady state experiments. See, however, ref 21.
- (29) W. R. Ware, "Creation and Detection of the Excited State", A. A. Lamola, Ed., Marcel Dekker, New York, N.Y., 1971.
- (30) C. Lewis, W. R. Ware, L. J. Doemeny, and T. L. Nemzek, *Rev. Sci. Instrum.*, **44**, 107 (1973).